CRYSTAL GROWTH & DESIGN

pubs.acs.org/crystal

Article

Effect of Different Evaporation Rates on Gypsum Habit: Mineralogical Implications for Natural Gypsum Deposits

Andrea Cotellucci,* Luca Pellegrino, Emanuele Costa, Marco Bruno, Francesco Dela Pierre, Dino Aquilano, Enrico Destefanis, and Linda Pastero

Cite This: *Cryst. Growth Des.* 2023, 23, 9094−9102

Read Online

ACCESS | Metrics & More | Article Recommendations | Supporting Information

ABSTRACT: When a solution saturated in $CaSO_4{\cdot}2H_2O$ evaporates at room temperature, gypsum crystals precipitate with both single and twinning habits. However, the twinning laws of gypsum involved in this process have long been debated. Recently, easy steps have been described to univocally recognize the twinning laws of gypsum. Therefore, in this study, we have replicated evaporation experiments and focused on identifying these twinning laws. Different precipitation frequencies of gypsum crystals with (i) curved habits and (ii) twins, according to the 100 and $\bar{1}01$ penetration twinning laws, have been observed as the evaporation rate increased. The crystal aspect ratio (length/width crystal ratio) might serve as a quick measure for distinguishing between 100 and $\bar{1}01$ penetration twinning laws, and the occurrence of these twinning laws in sedimentary environments is suggested. Moreover, high evaporation rates promote curved crystals with both symmetric and asymmetric habits. Based on crystallographic considerations, the asymmetric habit might be explained by a homoepitaxial mechanism, where systematic rotations of the common 2D coincidence cells occur. These results describe which of the twinning laws of gypsum are possible in a pure solution and, for the first time, establish a correlation between different gypsum habits and different evaporation rates, contributing to a better understanding of gypsum habit in evaporitic environments.

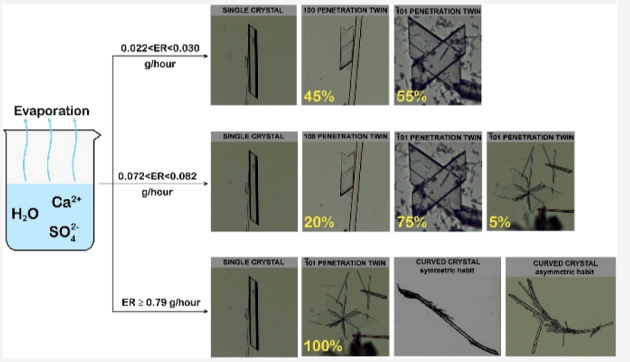

1. INTRODUCTION

Gypsum (calcium sulfate dihydrate, $CaSO_4{\cdot}2H_2O$) is the most abundant sulfate mineral on Earth's surface[1] and it is found in a wide range of natural and anthropogenic environments, such as hypersaline lakes, sabkhas and saltworks,[2−4] soils,[5] desertic regions,[6] and caves.[7,8] Noteworthy, widespread gypsum deposition occurred in the geological past, such as in the Paratethys and Mediterranean basins during the Middle and Late Miocene, respectively.[9,10] Furthermore, gypsum deposits have also been detected on Mars[11,12] and a swallowtail gypsum habit, commonly referred to gypsum twins,[13] has been recently observed by the NASA's Curiosity Mars rover.[14]

Gypsum is characterized by single and twinning crystals. Single crystals show acicular, tabular, prismatic, and lenticular habits. In some cases, gypsum can also form distinctive curved crystal structures such as the ram's horn gypsum found in caves,[7,15] and sabre gypsum observed in Badenian evaporitic gypsum deposits.[16] Twinning is an epitaxial phenomenon that involves a regular mutual orientation between two crystals of the same phase: the parent (P) and twinned (T) crystals.[17] Twinning crystals are the result of a symmetry operation, also called "twin operation" (e.g., mirror plane, inversion center), of the crystal structure with respect to a specific plane: the twinning law.[18] Twinning occurs under conditions of supersaturation, where a crystallization unit (an atom or group of atoms) takes energy such that a second individual is generated, twinned with respect to the original crystal. This crystallization unit can be temporarily blocked by subsequent deposition units and then proceeds to grow, resulting in a second twinned crystal. In terms of their genesis, gypsum twins are categorized as *growth twins*, formed during the crystal growth process. Other categories include *transformation twins*, formed following a phase transition, where symmetry elements lost in the transition act as twin elements, and *mechanical or gliding twins*, which result from structural shear in plastic deformation. Both the oriented attachment and classical nucleation mechanisms for the formation of *growth twins* have been described.[19] However, experiments are lacking, to date, aimed at elucidating whether the oriented attachment or the classical nucleation mechanisms are involved in the formation of gypsum twinning crystals.

Received: September 22, 2023
Revised: October 30, 2023
Accepted: October 31, 2023
Published: November 10, 2023

Due to structural constraints, five twinning laws are possible for gypsum and the P−T individuals are mutually related by one of the following twinning operations: rotation of 180°, mirror plane, or inversion center.[20] Moreover, each twinning law of gypsum is described by a contact and penetration twinning mechanism.[21,22] Thus, gypsum may show at least ten different twinning habits.

Since the pioneering studies of Lacroix,[23] such a wide array of habits was believed to reflect peculiar growth conditions. A better understanding of the environmental factors responsible for different gypsum habits may have crucial implications for the interpretation of the origin of the gypsum deposits formed in the geological past.

To recognize the effect of impurities on the gypsum habit, the impurity-free gypsum habit must be known. This is often reported in the literature by mixing calcium chloride dihydrate ($CaCl_2{\cdot}2H_2O$) or calcium nitrate ($Ca(NO_3)_2$) with sodium sulfate (Na_2SO_4) to produce supersaturated solutions with respect to calcium sulfate dihydrate ($CaSO_4{\cdot}2H_2O$).[13,24,25] This approach mostly produces acicular crystals.[26,27] Unfortunately, Na^+ ions affect the nucleation, growth kinetic and habit of gypsum crystals, and are incorporated into the crystals.[28] Therefore, this synthesis does not reflect the habit of gypsum grown in a pure system, since it contains sodium chloride or nitrate coming from reagents.

Other experiments have been designed to obtain gypsum crystals from a pure solution including (a) the hydration of bassanite,[29] and (b) the evaporation of a solution saturated in $CaSO_4{\cdot}2H_2O$.[13,30] In these experiments, twinning crystals were commonly detected. However, the identification of their twinning laws has been debated[13] because of the limited knowledge of the morphological, crystallographic, and optical characteristics of the five twinning laws of gypsum. Kern and Rehn,[29] as well as Simon,[30] argued that both 100 and $\bar{1}01$ penetration twinning laws of gypsum are usual in pure aqueous solution, with the $\bar{1}01$ penetration twinning law being the more prevalent of the two. In contrast, Cody and Cody[13] concluded that the $\bar{1}01$ penetration twinning law recognized in previous works[29,30] were 100 twins instead.

To date, the crystallographic growth directions of the five twinning laws have been described and their twinning energies determined.[21,22] Moreover, Cotellucci et al.[31] provided new and useful tools to recognize the different twinning laws of gypsum univocally. Therefore, we believe that reinvestigating gypsum habit in a pure system is needed, focusing on the identification of twinning laws and their habit descriptions.

As mentioned above, starting from a solution saturated in $CaSO_4{\cdot}2H_2O$, when evaporation occurs, gypsum crystals precipitate. Remarkably, gypsum precipitation by evaporation is the most common phenomenon in natural environments and the most easily reproducible process in the laboratory. Moreover, by modifying the evaporation rate (ER, hereinafter), it is possible to observe whether and how the gypsum habit changes.

Here, we have replicated evaporation experiments, paying attention to the ER, that is, a pure solution saturated in $CaSO_4{\cdot}2H_2O$ has been left to evaporate at different ERs. Acicular single crystals, curved crystals, and twins showing the 100 and $\bar{1}01$ penetration twinning laws have been observed. Our results, based on the precipitation frequencies, indicate that the occurrence of the 100 penetration twinning law decreases with increasing ER, whereas the opposite is true for the $\bar{1}01$ penetration twinning law. Furthermore, two different habits related to the $\bar{1}01$ penetration twinning law have been detected: a "cruciform" habit with a visible compenetration between the parent and twinned crystals and a "butterfly" one where the compenetration is not visible. The formation of 100 and $\bar{1}01$ penetration twinning laws is also promoted by tannic acids and α-amylase enzyme, which are commonly found in sedimentary environments;[32,33] hence, both types of penetration twins may occur in evaporitic-sedimentary environments. Moreover, the crystal aspect ratio (length/width crystal ratio, AR hereinafter) could potentially serve as a quick and useful tool for distinguishing between 100 and $\bar{1}01$ penetration twins. However, it is important to acknowledge that more rigorous analyses are available for distinguishing between these two twinning laws.[31]

Previous crystal growth experiments have associated the curved habit of gypsum with specific impurities dissolved in the solution.[34,35] Moreover, our findings suggest that high ER can also promote the curvature, and a homoepitaxial mechanism may be involved in the formation of the asymmetric curved habit.

2. MATERIAL AND METHODS

$CaSO_4{\cdot}2H_2O$ reagent plus (≥99% Sigma-Aldrich) and ultrapure water (18 MΩ; obtained using an Elga PURELAB Flex3 water purification system) have been used to prepare a $CaSO_4{\cdot}2H_2O$ saturated solution at room temperature (20 °C). Evaporation experiments have been performed at 20, 30, and 40 °C. The related $CaSO_4{\cdot}2H_2O$ solubility values, as well as the conductivity, have been calculated using PHREEQC v3.6.3 version[36] and the default phreeqc database.

$CaSO_4{\cdot}2H_2O$ saturated solution has been prepared by adding 5.0 g/L of $CaSO_4{\cdot}2H_{2O(s)}$ to water, exceeding the gypsum saturation in pure water (2.54 g/L at 20 °C). Then, $CaSO_4{\cdot}2H_{2O(s)}$ was kept stirring in the flask for 15 days to ensure saturation. Solution saturation has been verified by conductivity measurements; when the conductivity value does not change significantly, saturation is reached. We have measured 2030 μS/cm as a stable value, slightly higher than the theoretical one (i.e., 2000 μS/cm). The solution pH was 5.4 and measured with a HANNA HI211 pH meter. Therefore, the solution was filtered using a cellulose filter with a pore size of 0.45 μm to remove any $CaSO_4{\cdot}2H_2O$ particles.

Four different experimental conditions have been investigated (G1−G4) and for each condition, three replicas have been carried out. The maximum and minimum values of evaporation rates associated with each experimental condition are given in the main text; see Figures S1−S4 for the evaporation rate associated with each replica:

i In G1, ≈30 g of solution has been stored in a 5 cm diameter beaker, covered with a perforated parafilm, and allowed to evaporate at room temperature (0.022 < ER < 0.030 g/h).
ii In G2, ≈30 g of solution has been stored in a 5 cm diameter beaker, without the parafilm cover, and allowed to evaporate at room temperature (0.072 < ER < 0.082 g/h).
iii In G3, ≈30 g of solution has been stored in a 5 cm diameter beaker, and allowed to evaporate in a ventilated oven at 30 °C (0.79 < ER < 1.05 g/h).
iv In G4, ≈30 g of solution has been stored in a 5 cm diameter beaker, and allowed to evaporate in a ventilated oven at 40 °C (1.59 < ER < 1.94 g/h).

For each experiment, the evaporation rate was calculated by measuring the weight of the solution at different times with an analytical laboratory balance, with precision until the tenth of a milligram. However, we have considered only the values up to the second decimal place. Due to evaporation, the third and fourth decimal places did not provide stable values, especially in G3 and G4 solutions in which the beaker has been, each time, kept out of the oven, the weight rapidly sampled, and then reinserted into the oven to limit the cooling of the solution.

https://doi.org/10.1021/acs.cgd.3c01124
Cryst. Growth Des. 2023, 23, 9094−9102

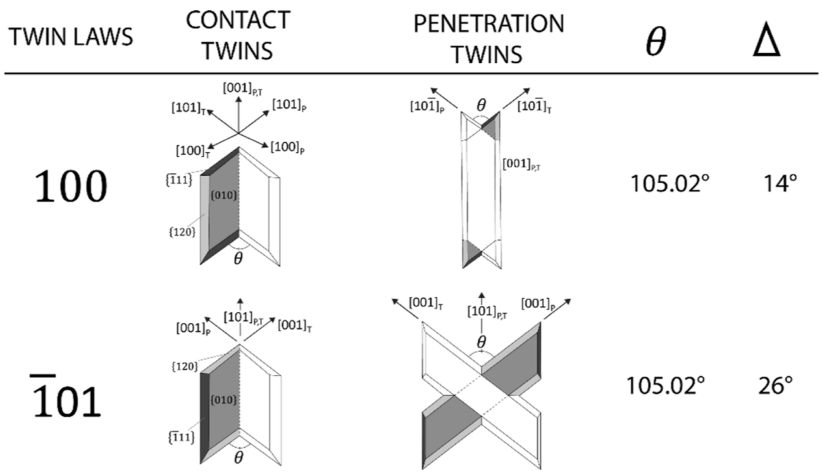

Figure 1. Geometry of the 100 and $\bar{1}01$ contact and penetration twins viewed along the [010] direction of gypsum. Reproduced from refs 21 and 22. Copyright 2012 American Chemical Society. For each twin law, the re-entrant angle value (θ) and the optical extinction angle value (Δ) have been reported. Subscripts "P" and "T" identify the two individuals, parent and twinned, making the twin.

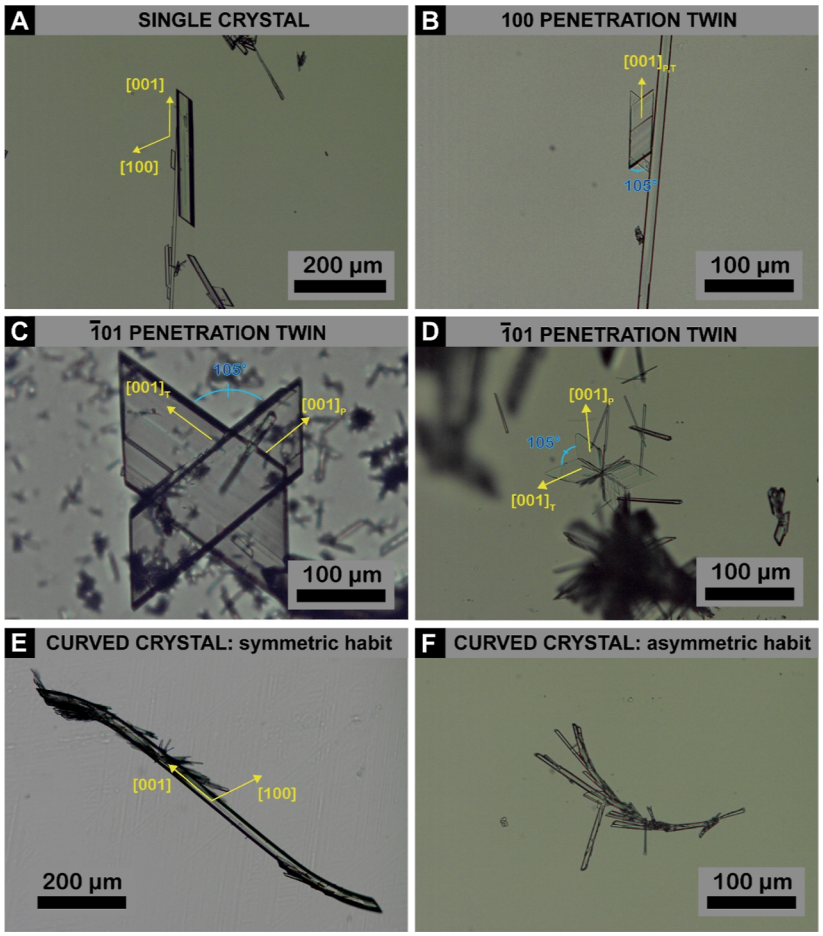

Figure 2. Gypsum habits were detected in G1−G4 experiments. A re-entrant angle of 105° identifies both 100 and $\bar{1}01$ twinning laws; two re-entrant angles at opposite sides identify a penetration twin.

When the temperature increases, gypsum solubility slightly increases as well and, thus, G3 and G4 solutions are slightly unsaturated with respect to $CaSO_4{\cdot}2H_2O$. From 20 to 30 °C the solubility increases by ~0.09 g/L (2.63 g/L at 30 °C), whereas at 40 °C the solubility increases by 0.12 g/L (2.66 g/L at 40 °C). If we consider the lowest evaporation rate among those measured in G3 and G4 experimental conditions, after 6.8 and 4.5 min the saturation is rereached in G3 and G4, respectively, corresponding to a loss of 89.5 mg (G3) and 112.5 mg (G4). Hence, increasing the temperature from 20 to 30 (or 40 °C) does not significantly affect gypsum solubility, for our purposes at least.

Solutions were allowed to evaporate up to about half of the sample weight. Precipitated crystals have been recovered and washed with ultrapure water, dried overnight at room temperature, and then analyzed by optical (Olympus BX4 with JENOPTIC ProgResC5 digital camera) and electron microscopy (JEOL-JSM-IT300LV-SEM),

https://doi.org/10.1021/acs.cgd.3c01124
Cryst. Growth Des. 2023, 23, 9094−9102

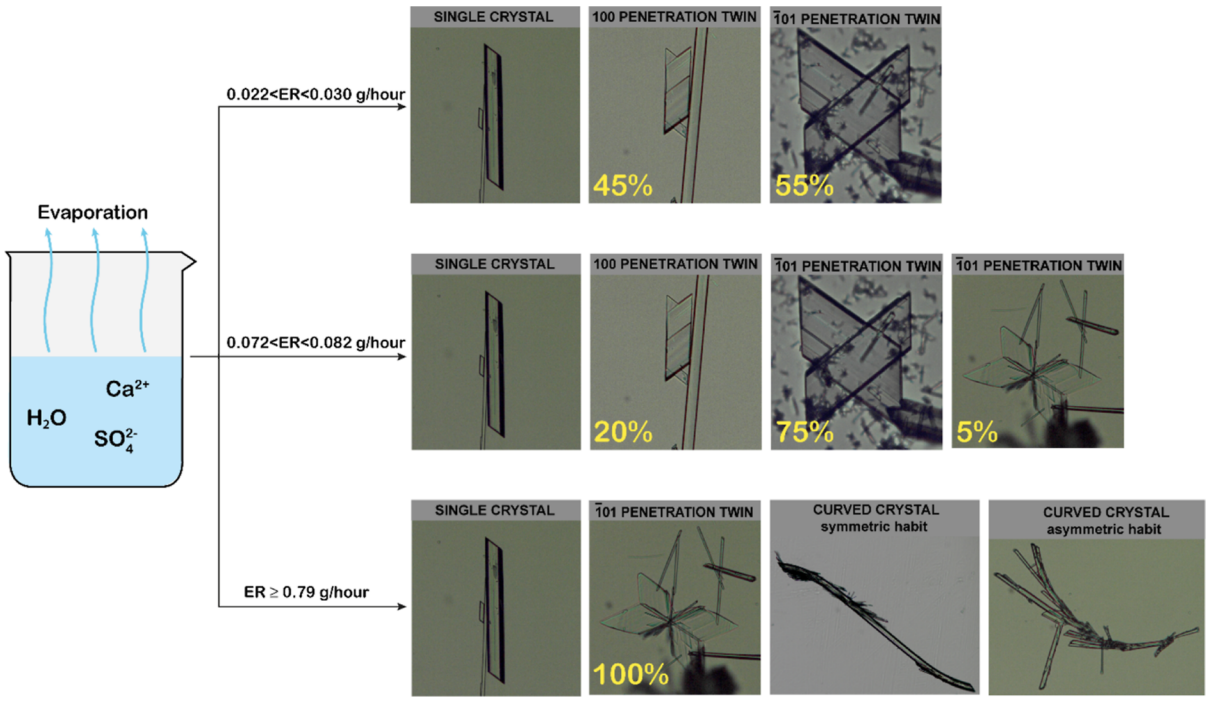

Figure 3. Gypsum crystal habits and twinning laws precipitation frequencies as a function of ERs. For the sake of simplicity, the percentage values shown in the figure were approximated to unity. Refer to the main text for values approximated to the first decimal place.

equipped with secondary electrons and backscattered electrons (SE and BSE, respectively) detectors, and energy-dispersive X-ray spectrometer.

From the evaporation of the G1−G4 solutions, both single and twinning habits of gypsum crystals have been obtained. The related twinning laws have been identified by measuring the extinction angle with the optical microscope using crossed polarizers as described in Cotellucci et al.[31]

Fifty optical images of gypsum twins have been taken and analyzed using ImageJ image processing software, and their AR was calculated (Figure S5; Table S1). For each experimental condition, the precipitation frequencies of the different twinning laws have been measured based on 80 twins detected in each replica. The average percentage value of these measurements is reported in the main text, along with the absolute error.

Historically, gypsum was indexed in a variety of nearly equivalent ways.[37−39] A comparison of these different indexing has been presented by Aquilano et al.[1] Here, we have adopted the monoclinic $C2/c$ space group where a_0 = 5.63, b_0 = 15.15, c_0 = 6.23 Å; $\alpha = \gamma = 90°$; $\beta = 113.50°$.[40] Our choice has been grounded in two practical reasons:

I This frame uses the smallest lattice vectors;

II The [001] ≡ z axis coincides with the morphological elongation of the crystals growing from pure aqueous solution and of the natural crystals' majority.

3. RESULTS AND DISCUSSION

3.1. Effect of Different Evaporation Rates on Gypsum Habit. Five different twinning laws are known for gypsum.[20] Geometrically, each twinning law is characterized by a specific re-entrant angle value. In addition, a re-entrant angle and an arrowhead one at opposite sides indicate a contact twin, while two re-entrant angles observed at opposite twinning sides identify a penetration twin.[21,22] Unfortunately, the 100 and $\bar{1}$01 twinning laws share the same re-entrant angle value (θ) of 105°. Thus, we cannot use this value alone to distinguish these twins. The formal way to identify the 100 and $\bar{1}$01 twinning laws should require the measurement of the extinction angle between the two individuals forming the twins (Δ) by means of optical microscopy in crossed polarizers. Such an angle is 14 and 26° for 100 and $\bar{1}$01 twin law, respectively.[31] Figure 1 provides an overview of the theoretical geometry of the 100 and $\bar{1}$01 twinning laws. A more detailed description of the morphological, optical, and structural characteristics of the five twinning laws of gypsum can be found elsewhere in the literature.[1,20−22,31] Moreover, recent investigations have shown that in 100 contact twins the subcrystals making the twin are parallel to the twinning plane, whereas in $\bar{1}$01 contact twins the subcrystals are obliquely elongated with respect to the twinning plane. The growth direction of the primary fluid inclusions follows that of the subcrystals making the twin. Therefore, in addition to the extinction angle, both the subcrystals and fluid inclusion growth directions are useful tools to distinguish the 100 from the $\bar{1}$01 twinning laws.[31]

At the slowest evaporation rate (G1 solution: 0.022 < ER < 0.030 g/h), single crystals [001] elongated, 100 penetration twins, and $\bar{1}$01 penetration twins have been detected (Figure 2A−C). The precipitation frequencies of 100 and $\bar{1}$01 gypsum twinning laws are as follows: 45.4 ± 1.8% for the 100 penetration twinning law and 54.6 ± 1.8% for the $\bar{1}$01 penetration one. When increasing the evaporation rate (G2 solution: 0.072 < ER < 0.082 g/h), we have obtained the precipitation of acicular crystals, and twinned crystals showing the 100 and $\bar{1}$01 penetration twinning laws (Figure 2A−D). $\bar{1}$01 penetration twinning law shows two different habits: the "cruciform" habit with a visible compenetration between the two individuals forming the twin, already detected in G1 solution (Figure 2C), and a "butterfly" one with a not visible compenetration (Figure 2D). In addition, the precipitation frequencies of the twinning laws slightly changed with respect to the G1 solution: 19.6 ± 3.8% for the 100 penetration twinning law, 75.8 ± 3.8% for the $\bar{1}$01 penetration twinning law with a cruciform habit, and 4.6 ± 1.3% for the $\bar{1}$01

https://doi.org/10.1021/acs.cgd.3c01124
Cryst. Growth Des. 2023, 23, 9094−9102

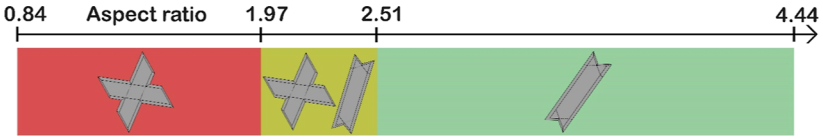

Figure 4. Distribution of the 100 and $\bar{1}01$ penetration twinning laws as a function of the aspect ratio. Red: range of aspect ratio where only $\bar{1}01$ penetration twins have been observed; yellow: range of aspect ratio where both 100 and $\bar{1}01$ penetration twins have been measured; green: range of aspect ratio where only 100 penetration twins have been observed.

penetration "butterfly" twinning law. At higher evaporation rates (ER $\geq$ 0.79 g/h), we have obtained the precipitation of acicular crystals, the $\bar{1}01$ penetration twinning law with butterfly habit, and curved crystals (Figure 2A,D–F). 100 penetration twinning law and $\bar{1}01$ penetration twinning law with cruciform habit have not been detected. Curved crystals exhibit both "symmetric" (Figure 2E) and "asymmetric" curvature (Figure 2F). The occurrence of different gypsum crystal habits and precipitation frequencies of twinning laws as a function of ERs are sketched in Figure 3.

Based on these findings, the precipitation frequencies of both 100 and $\bar{1}01$ penetration twins depend on the evaporation rate, and the $\bar{1}01$ penetration twinning law can precipitate with two different habits (Figure 2C,D), whose precipitation frequency is related to the evaporation rate as well.

Using the rich statistical data on the penetration growth twins described in the literature, Massaro et al.[22] calculated the different habits of penetration twins. They observed that the 100 penetration twinning habit is more elongated when compared to the $\bar{1}01$ penetration one and, thus, the AR should be a fast and useful parameter to distinguish these twinning laws. To test this hypothesis, we have measured the AR of fifty 100 and $\bar{1}01$ penetration twins (Figure S5; Table S1). Based on this data set, only 100 penetration twins have shown an AR $> 2.51 \pm 0.02$, whereas exclusively $\bar{1}01$ penetration twins show an AR $< 1.97 \pm 0.01$ (Table S2; Figure 4). In the range $1.97 <$ AR < 2.51, the aspect ratio of both 100 and $\bar{1}01$ penetration twinning laws are measured and thus this range does not allow to distinguish between the two. Therefore, the AR parameter might be a fast and useful tool to distinguish between 100 and $\bar{1}01$ penetration twins, in addition to those already described in Cotellucci et al.[31]

The curved habit of gypsum, also known as "bent habit", has already been reported in the literature.[34,35] To our knowledge, two different experimental growth conditions can promote the curvature in gypsum crystals: diffusion-controlled experiments in the presence of impurities, and evaporation experiments in the presence of impurities.[34] The proposed formation mechanism suggests that impurity absorption triggers structural defects and crack formations in gypsum during crystal growth.[34,35] It has been proposed that cracks and defects promote the nucleation and growth of a new gypsum crystallite with a different crystallographic orientation with respect to the former crystal; as a result, the overall habit of the aggregated crystals at the growth front is bent, as shown in Figure 2E,F. Our experiments reveal another growth attribution to curved crystals, which occurs when a solution rich in Ca^{2+} and SO_4^{2-} ions rapidly evaporates without any dissolved additives. In this case, crack formation is promoted by a high ER. Indeed, as the rate of evaporation increases, it changes the rate at which the concentration of the solution increases. Consequently, the supersaturation value with respect to gypsum increases from the G1 to G4 solution. According to the classical nucleation theory, the nucleation rate, that is, the number of crystals generated in a supersaturated system, is proportional to the supersaturation value.[41] Moreover, the growth rate of a specific crystal surface depends on the supersaturation, and a higher growth rate promotes a higher density of defects.[42] Hence, the high evaporation rates we observed promoted high supersaturation values, accelerated crystal growth rates, and hence increased crystal defectivity. This, as observed in curved crystals grown in the presence of impurities, promoted the nucleation and growth of new gypsum crystallites with different crystal orientations compared to the original crystal, ultimately giving rise to bending in the crystal habit. Importantly, our set of experiments has been conducted at different temperatures; hence, the bending could be related to an increase in evaporation rate, temperature, or a combination of both. Unfortunately, the specific effect of temperature on the gypsum habit has not been investigated yet. Specific and quantitative analyses should be carried out to provide reliable information about the temperature-gypsum habit relationship. Nonetheless, this type of investigation goes beyond the scope of this work, and we envisage that future work will further investigate this relationship. Against the involvement of temperature in promoting the curvature, we point out that in diffusion-controlled growth experiments, curved crystals have been obtained at room temperature,[35] and Rinaudo et al.[34] observed the curvature at 25, 35, and 45 °C. Moreover, different growth experiments dealt with gypsum precipitation at temperatures ranging between 5 and 60 °C (although many other variables were involved), but curved crystals have never been described.[32,43] Therefore, we can provisionally assume that the temperature is not involved in promoting the curvature, but rigorous analyses are needed.

Finally, it is pivotal to note that the curved habit of gypsum is not only an artifact of crystal growth of laboratory experiments but is observed in natural environments too.[7,15,16] Based on the findings described here, we suggest considering the evaporation rate as a plausible parameter in promoting the curved habit in natural environments overall in evaporitic settings.

3.2. Hypothetical Morphogenetic Mechanism of the Asymmetric Curvature. Intriguingly, in the symmetric "curved" habit the two curvatures are symmetrically related by means of a rotation of 180° or an inversion center. Hence, Rinaudo et al.[34] have suggested a twinning mechanism, promoted by cracks formation, to explain the observed habit. However, only crystallographic considerations have been carried out, and thus, further computational and experimental analyses should be performed to strengthen this growth model.

In contrast, the asymmetrically curved habit shown in Figure 2F cannot be explained by a twinning mechanism because there is not a twin operation related to the growth shape.[44,45] This habit arises from the overlapping of crystals with different orientations (from 8 to 25°) between the direction of one crystal and its neighbor (Figure 5). To explain this crystal

https://doi.org/10.1021/acs.cgd.3c01124
Cryst. Growth Des. 2023, 23, 9094−9102

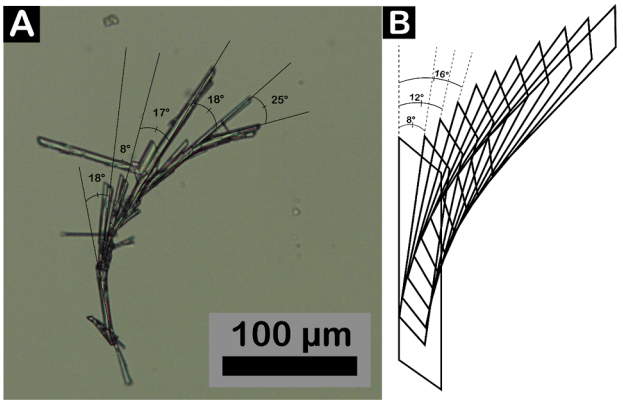

Figure 5. (A) The angular misfit between the direction of one crystal and its next/previous one composing the asymmetric curved habit ranges between 8 and 25°. The reported angular values should be interpreted as an approximation of the true angle value since they have been measured manually with ImageJ image processing software. A confidence interval of ±2° should be considered. (B) Sketch of the curvature. A small angular misfit between the direction of one crystal and its neighbor produces a curved habit.

curvature, a homoepitaxial mechanism may be involved, where systematic rotations of the common 2D coincidence cells occur. This growth mechanism does not require a twin operation. Indeed, in a homoepitaxial mechanism two or more crystallographic forms {*hkl*} and {*h*′*k*′*l*′}, of the same crystal species, can associate in an epitaxial relation without producing a new twinning law.[17] Referred to curved crystals, the crystallographic forms involved in the homoepitaxy could be the {010}, {120}, or generally, the {1*k*0},[46] considering crystals are compenetrated one each other; therefore, crystallographic forms (not detectable by imaging) could be involved (Figure 6). We have investigated the 2D coincidence cells

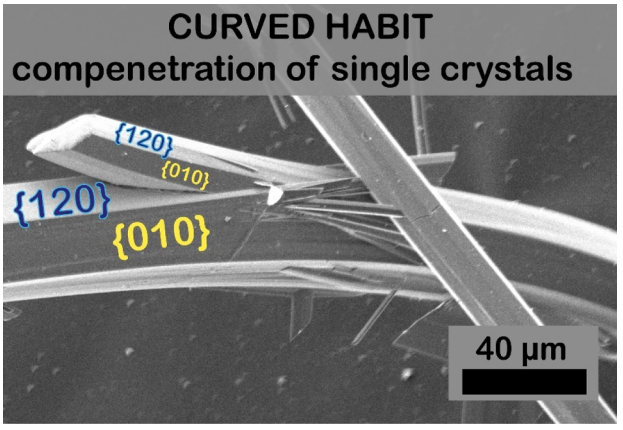

Figure 6. Crystals composing the curved habit cross one another, sharing the {010} and the {120} crystallographic forms.

occurring between two (010) planes, by rotating one plane up from 8 to 25°. Geometrically, we have found that there are many different positions coherent with the constraints required for epitaxy interaction (i.e., linear and area misfit <14%) (Table 1).[47] The multitude of 2D coincidence cells satisfying epitaxial constraints agrees with the angular misfit variety measured on our curved crystals; therefore, a homoepitaxial mechanism may be involved in the formation of the asymmetric curved habit. However, more in-depth analyses are required to validate this hypothesis.

Table 1. 2D Coincidence Cells of Two 010 Planes Rotating One Plane up from 8 to 25°[a]

rotation angle (deg)	directions	linear misfit (%)	area misfit (%)
8	[307]≡[207]	−1.2	3.5
	[702]≡[703]	+0.8	
9	[306]≡[206]	−0.4	<1.0
	[702]≡[703]	+0.8	
10	[306]≡[206]	−0.4	<1.0
	[702]≡[703]	+0.8	
11	[305]≡[205]	+1.0	≈0
	[702]≡[703]	+0.8	
12	[305]≡[205]	+1.0	≈0
	[602]≡[603]	−1.3	
13	[204]≡[104]	−1.4	≈16.5
	[501]≡[502]	−15.2	
14	[204]≡[104]	−1.4	≈16.5
	[501]≡[502]	−15.2	
15	[204]≡[104]	−1.4	≈0
	[401]≡[402]	−0.5	
16	[204]≡[104]	−1.4	≈0
	[401]≡[402]	−0.5	
17	[203]≡[103]	+2.0	<1.0
	[401]≡[402]	−0.5	
18	[203]≡[103]	+2.0	<1.0
	[401]≡[402]	−0.5	
19	[203]≡[103]	+2.0	<1.0
	[401]≡[402]	−0.5	
20	[203]≡[103]	+2.0	<1.0
	[401]≡[402]	−0.5	
21	[203]≡[103]	+2.0	<1.0
	[401]≡[402]	−0.5	
22	[305]≡[105]	−1.5	≈0%
	[601]≡[603]	+1.2	
23	[102]≡[002]	−9.5	≈2.0
	[$\bar{1}$02]≡[$\bar{2}$01]	+4.2	
24	[102]≡[002]	−9.5	≈1.0
	[$\bar{1}$02]≡[$\bar{2}$01]	+4.2	
25	[102]≡[002]	−9.5	≈8.5
	[$\bar{5}$03]≡[$\bar{7}$00]	+0.2	

[a]Only for a rotation of 13 and 14° the constraints required for epitaxy (i.e., linear and area misfit <14%) are not satisfied.

3.3. Mineralogical Implication: Do the "Swallowtail" Gypsum Twins Represent Different Twin Laws? Gypsum precipitation *via* evaporation was a common process in ancient sedimentary basins involved in the evaporitic events that punctuated the Earth hystory.[48] Notwithstanding, 100 and $\bar{1}$01 penetration twins have never been identified in the sedimentary successions deposited in response to these dramatic modifications of the basin hydrologic balance. These complex chemical environments rich in organic and inorganic compounds deriving, for instance, from both planktonic and benthonic biological activity[49−51] may have selected different twinning laws of gypsum with respect to the 100 and $\bar{1}$01 penetration ones. However, crystal growth experiments claim that specific organic molecules commonly found in sedimentary environments (tannic acid, deriving from the decomposition of plant leaves; α-amylase, an enzyme excreted into soils and water by bacteria, fungi, algae, and plant roots) promote the formation of 100 and $\bar{1}$01 penetration

https://doi.org/10.1021/acs.cgd.3c01124
Cryst. Growth Des. 2023, 23, 9094−9102

twinning laws.[32,33] Therefore, there is apparently no valid reason that 100 and $\bar{1}01$ penetration twins cannot be observed in modern and ancient sedimentary successions. We propose that 100 and $\bar{1}01$ penetration twins have been observed in nature but inappropriately defined as "swallowtail twins", which is the terminology commonly used to identify gypsum twinned crystals with a shape similar at first glance similar. Recently, straightforward and reliable methods have been proposed to geometrically and univocally recognize the different twinning laws of gypsum.[31] Therefore, we strongly suggest improving the identification of the different gypsum twinning laws observed in nature, as they can serve as a proxy for the chemistry of the original water from which gypsum precipitated,[31,33] hence contributing to the interpretation of the gypsum depositional environment in ancient deposits.

4. CONCLUSIONS

In this study, the effect of evaporation rate on gypsum habit was investigated by carrying out four batches of experiments at four different evaporation rates: different gypsum habits as a function of evaporation rates have been detected.

By increasing the evaporation rate, the formation of the $\bar{1}01$ penetration twinning law is favored with respect to the 100 penetration one, and the $\bar{1}01$ penetration twinning law can occur with two different habits whose precipitation frequencies are related to the evaporation rate as well. Previous experiments disclosed the formation of 100 and $\bar{1}01$ twinned gypsum crystals in the presence of organic molecules characteristics of sedimentary environments.[32,33] Consequently, these twinning laws can be detected in evaporitic-sedimentary environments. Aimed at favoring researchers to identify the twinning laws of gypsum crystals, we have proposed the measurement of crystal aspect ratio (length/width crystal ratio) as a potentially fast and useful tool to distinguish between 100 and $\bar{1}01$ penetration twins.

At higher evaporation rates (ER $\geq$ 0.79 g/h), curved crystals exhibit both "symmetric" and "asymmetric" curvatures. Based on crystallographic considerations, Rinaudo et al.[34] suggested a twinning mechanism may promote the symmetric curvature, whereas we have hypothesized a homoepitaxial mechanism for the asymmetric one. Moreover, until today, the crystal curvature has been related to impurities absorption,[34,35] but another growth attribution has been here documented, independent from the chemical environment and only related to supersaturation.

To summarize, these experimental findings provide the first evidence of different gypsum habits as a function of evaporation rates in a pure system. Acicular single crystals, curved crystals, and 100 and $\bar{1}01$ penetration twins are the habits detected. When the effect of additives on gypsum habits is explored by performing crystal growth experiments, and when different gypsum habits are analyzed in evaporitic environments, this wide array of habits should be considered.

■ ASSOCIATED CONTENT

Supporting Information

The Supporting Information is available free of charge at https://pubs.acs.org/doi/10.1021/acs.cgd.3c01124.

Evaporation rates associated with each experimental condition, and aspect ratio measurements on both 100 and $\bar{1}01$ penetration twins (PDF)

■ AUTHOR INFORMATION

Corresponding Author

Andrea Cotellucci − *Department of Earth Sciences, University of Turin, 10124 Torino (TO), Italy;* orcid.org/0000-0003-2027-3260; Phone: +390116705126; Email: andrea.cotellucci@unito.it

Authors

Luca Pellegrino − *Department of Earth Sciences, University of Turin, 10124 Torino (TO), Italy*

Emanuele Costa − *Department of Earth Sciences, University of Turin, 10124 Torino (TO), Italy*

Marco Bruno − *Department of Earth Sciences, University of Turin, 10124 Torino (TO), Italy; NIS, Centre for Nanostructured Interfaces and Surfaces, University of Turin, 10135 Torino (TO), Italy;* orcid.org/0000-0002-0161-574X

Francesco Dela Pierre − *Department of Earth Sciences, University of Turin, 10124 Torino (TO), Italy*

Dino Aquilano − *Department of Earth Sciences, University of Turin, 10124 Torino (TO), Italy;* orcid.org/0000-0002-3908-928X

Enrico Destefanis − *Department of Earth Sciences, University of Turin, 10124 Torino (TO), Italy*

Linda Pastero − *Department of Earth Sciences, University of Turin, 10124 Torino (TO), Italy; NIS, Centre for Nanostructured Interfaces and Surfaces, University of Turin, 10135 Torino (TO), Italy;* orcid.org/0000-0002-9453-9503

Complete contact information is available at: https://pubs.acs.org/10.1021/acs.cgd.3c01124

Author Contributions

The manuscript has been written through contributions of all authors. All authors have given approval to the final version of the manuscript.

Funding

PRIN 2017, of the Italian Ministry for Education, University and Research (MIUR) (grant no. 2017L83S77).

Notes

The authors declare no competing financial interest.

■ ACKNOWLEDGMENTS

We thank Davide Bernasconi (Department of Earth Sciences, University of Torino) for broadening article perspectives with his useful suggestions; Simone Aveni (Department of Earth Sciences, University of Torino) for his advice on data analysis; and Caterina Caviglia (Department of Earth Sciences, University of Torino) for providing technical support during laboratory experiments.

■ ABBREVIATIONS

ER, evaporation rate; AR, aspect ratio, length-width crystal ratio

■ REFERENCES

(1) Aquilano, D.; Otálora, F.; Pastero, L.; García-Ruiz, J. M. Three study cases of growth morphology in minerals: Halite, calcite and gypsum. *Prog. Cryst. Growth Charact. Mater.* **2016**, *62*, 227−251.

(2) Warren, J. K. The hydrological setting, occurrence and significance of gypsum in late Quaternary salt lakes in South Australia. *Sedimentology* **1982**, *29*, 609−637.

(3) Ortí, F. Selenite facies in marine evaporites: a review. *Quaternary Carbonate and Evaporite Sedimentary Facies and Their Ancient Analogues*; John Wiley & Sons, 2010; pp 431−463.
(4) Otálora, F.; Criado-Reyes, J.; Baselga, M.; Canals, A.; Verdugo-Escamilla, C.; García Ruiz, J. M. Hydrochemical and Mineralogical Evolution through Evaporitic Processes in Salar de Llamara Brines (Atacama, Chile). *ACS Earth Space Chem.* **2020**, *4*, 882−896.
(5) Jafarzadeh, A. A.; Burnham, C. P. Gypsum crystals in soils. *J. Soil Sci.* **1992**, *43*, 409−420.
(6) Shahid, S.; Abdelfattah, M. Gypsum Polymorphism in the Desert Environment of Abu Dhabi Emirate. *Eur. J. Sci. Res.* **2009**, *29*, 237−248.
(7) Wenrich, K. J.; Sutphin, H. B. Grand Canyon caves, breccia pipes and mineral deposits. *Geol. Today* **1994**, *10*, 97−104.
(8) García-Ruiz, J. M.; Villasuso, R.; Ayora, C.; Canals, A.; Otálora, F. Formation of natural gypsum megacrystals in Naica, Mexico. *Geology* **2007**, *35*, 327−330.
(9) Babel, M. Selenite-gypsum microbialite facies and sedimentary evolution of the Badenian evaporite basin of the northern Carpathian Foredeep. *Acta Geol. Pol.* **2005**, *55*, 187−210.
(10) Natalicchio, M.; Pellegrino, L.; Clari, P.; Pastero, L.; Dela Pierre, F. Gypsum lithofacies and stratigraphic architecture of a Messinian marginal basin (Piedmont Basin, NW Italy). *Sediment. Geol.* **2021**, *425*, 106009.
(11) Gendrin, A.; Mangold, N.; Bibring, J. P.; Langevin, Y.; Gondet, B.; Poulet, F.; Bonello, G.; Quantin, C.; Mustard, J.; Arvidson, R.; LeMouélic, S. Sulfates in Martian layered terrains: the OMEGA/Mars Express view. *Science* **2005**, *307* (5715), 1587−1591.
(12) Langevin, Y.; Poulet, F.; Bibring, J. P.; Gondet, B. Sulfates in the north polar region of Mars detected by OMEGA/Mars Express. *Science* **2005**, *307* (5715), 1584−1586.
(13) Cody, A. M.; Cody, R. D. SEM and polarization analyzes updating early light microscope studies related to {101} twin formation in gypsum. *J. Cryst. Growth* **1989**, *98* (4), 731−738.
(14) Edgar, L. A.; Fraeman, A.; Gupta, S.; Fedo, C.; Grotzinger, J. P.; Stack, K.; Bennett, K. A.; Sun, V. Z.; Banham, S.; Stein, N.; Edgett, K. S. A lacustrine environment recorded at Vera Rubin ridge: overview of the sedimentology and stratigraphy observed by the Mars Science Laboratory Curiosity Rover. *AGU Fall Meeting Abstracts*, 2018; Vol. *2018*, P41A-01.
(15) Panczner, W. D. *Minerals of Mexico*; Springer Science & Business Media, 2013.
(16) Bąbel, M.; Olszewska-Nejbert, D.; Nejbert, K.; Ługowski, D. The Badenian evaporative stage of the Polish Carpathian Foredeep: sedimentary facies and depositional environment of the selenitic Nida Gypsum succession. *Guidebook for Field Trips Accompanying IAS 31st Meeting of Sedimentology Held in Kraków on 22nd−25th of June 2015*, 2015; pp 25−50.
(17) Bruno, M.; Pastero, L.; Cotellucci, A.; Aquilano, D. Epitaxy: a methodological approach to the study of an old phenomenon. *CrystEngComm* **2022**, *24*, 4165−4173.
(18) Parsons, S. Introduction to twinning. *Acta Crystallogr., Sect. D: Biol. Crystallogr.* **2003**, *59* (11), 1995−2003.
(19) Nespolo, M.; Ferraris, G. The oriented attachment mechanism in the formation of twins-a survey. *Eur. J. Mineral.* **2004**, *16* (3), 401−406.
(20) Follner, S.; Wolter, A.; Helming, K.; Silber, C.; Bartels, H.; Follner, H. On the Real Structure of Gypsum Crystals. *Cryst. Res. Technol.* **2002**, *37*, 207−218.
(21) Rubbo, M.; Bruno, M.; Massaro, F. R.; Aquilano, D. The Five Twin Laws of Gypsum ($CaSO_4{\cdot}2H_2O$): A Theoretical Comparison of the Interfaces of the Contact Twins. *Cryst. Growth Des.* **2012**, *12*, 264−270.
(22) Rubbo, M.; Bruno, M.; Massaro, F. R.; Aquilano, D. The Five Twin Laws of Gypsum ($CaSO_4{\cdot}2H_2O$): A Theoretical Comparison of the Interfaces of the Penetration Twins. *Cryst. Growth Des.* **2012**, *12*, 3018−3024.
(23) Lacroix, A. *Minéralogie de la France et de ses colonies: description physique et chimique des minéraux, étude des conditions géologiques de leurs gisements*; Librairie Polytechnique: Baudry, 1986; Vol. *2*.
(24) Budz, J.; Jones, A. G.; Mullin, J. W. Effect of selected impurities on the continuous precipitation of calcium sulphate (gypsum). *J. Chem. Technol. Biotechnol.* **1986**, *36*, 153−161.
(25) De Vreugd, C. H.; Witkamp, G. J.; Van Rosmalen, G. M. Growth of gypsum III. Influence and incorporation of lanthanide and chromium ions. *J. Cryst. Growth* **1994**, *144*, 70−78.
(26) Rabizadeh, T.; Peacock, C. L.; Benning, L. G. Carboxylic acids: effective inhibitors for calcium sulfate precipitation? *Mineral. Mag.* **2014**, *78*, 1465−1472.
(27) Morales, J.; Astilleros, J. M.; Matesanz, E.; Fernández-Díaz, L. The Growth of Gypsum in the Presence of Hexavalent Chromium: A Multiscale Study. *Minerals* **2016**, *6*, 22.
(28) Rabizadeh, T.; Stawski, T. M.; Morgan, D. J.; Peacock, C. L.; Benning, L. G. The effects of inorganic additives on the nucleation and growth kinetics of calcium sulfate dihydrate crystals. *Cryst. Growth Des.* **2017**, *17*, 582−589.
(29) Kern, R.; Rehn, B. Etude expérimentale de la formation des macles de croissance du gypse. *C. R. Hebd. Seances Acad. Sci.* **1960**, *251*, 1300−1302.
(30) Simon, B. Contribution à l'étude de la Formation des Macles de Croissance. Ph.D. Dissertation, Department of Science, University of Aix-Marseille, France, 1968.
(31) Cotellucci, A.; Otálora, F.; Canals, À.; Criado-Reyes, J.; Pellegrino, L.; Bruno, M.; Aquilano, D.; Garcia-Ruiz, J. M.; Dela Pierre, F.; Pastero, L. 101 contact twins in gypsum experimentally obtained from calcium carbonate enriched solutions: mineralogical implications for natural gypsum deposits. *J. Appl. Crystallogr.* **2023**, *56*, 603−610.
(32) Cody, R. D.; Cody, A. M. Gypsum nucleation and crystal morphology in analog saline terrestrial environments. *J. Sediment. Res.* **1988**, *58*, 247−255.
(33) Cody, A. M.; Cody, R. D. Evidence for micro-biological induction of {101} Montmartre twinning of gypsum ($CaSO_4{\cdot}2H_2O$). *J. Cryst. Growth* **1989**, *98*, 721−730.
(34) Rinaudo, C.; Franchini-Angela, M.; Boistelle, R. Curvature of gypsum crystals induced by growth in the presence of impurities. *Mineral. Mag.* **1989**, *53*, 479−482.
(35) Punin, Y. O.; Artamonova, O. I. Autodeformation bending of gypsum crystals grown under the conditions of counterdiffusion. *Crystallogr. Rep.* **2001**, *46*, 138−143.
(36) Parkhurst, D. L.; Appelo, C. A. J. Description of Input and Examples for PHREEQC Version 3G Computer Program for Speciation, Batch-Reaction, One-Dimensional Transport and Inverse Geochemical Calculations. *US Geological Survey Techniques and Methods*; US Geological Survey, 2013; Vol. *6*, p 497.
(37) Cole, W. F.; Lancucki, C. J. A refinement of the crystal structure of gypsum $CaSO_4{\cdot}2H_2O$. *Acta Crystallogr., Sect. B: Struct. Crystallogr. Cryst. Chem.* **1974**, *30*, 921−929.
(38) Pedersen, B. F.; Semmingsen, D. Neutron diffraction refinement of the structure of gypsum, $CaSO_4{\cdot}2H_2O$. *Acta Crystallogr., Sect. B: Struct. Crystallogr. Cryst. Chem.* **1982**, *38*, 1074−1077.
(39) Comodi, P.; Nazzareni, S.; Zanazzi, P. F.; Speziale, S. High-pressure behavior of gypsum: A single-crystal X-ray study. *Am. Mineral.* **2008**, *93*, 1530−1537.
(40) Jong, W. F. d.; Bouman, J. Das reziproke und das Bravaissche Gitter von Gips. *Z. Kristallogr.-Cryst. Mater.* **1939**, *100*, 275−276.
(41) Otálora, F.; García-Ruiz, J. Nucleation and growth of the Naica giant gypsum crystals. *Chem. Soc. Rev.* **2014**, *43* (7), 2013−2026.
(42) Tsukamoto, K. In-situ observation of crystal growth and the mechanism. *Prog. Cryst. Growth Charact. Mater.* **2016**, *62* (2), 111−125.
(43) Cody, R. D. Growth and early diagenetic changes in artificial gypsum crystals grown within bentonite muds and gels. *Geol. Soc. Am. Bull.* **1976**, *87* (8), 1163−1168.

https://doi.org/10.1021/acs.cgd.3c01124
Cryst. Growth Des. 2023, 23, 9094−9102

(44) Pring, A. "Klein, C.; Hurlbut, C. S. Manual of Mineralogy (after James D. Dana) 21st ed.; John Wiley and Sons Inc., 1993". *Geol. Mag.* **1994**, *131* (5), 699−700.
(45) Nesse, W. D. *Introduction to Mineralogy*, 2nd; Oxford University Press, 2012.
(46) Massaro, F. R.; Rubbo, M.; Aquilano, D. Theoretical Equilibrium Morphology of Gypsum ($CaSO_4{\cdot}2H_2O$). 2. The Stepped Faces of the Main [001] Zone. *Cryst. Growth Des.* **2011**, *11*, 1607−1614.
(47) Mutaftschiev, B. *The Atomistic Nature of Crystal Growth*; Springer: Berlin, 2001; Vol. *43*.
(48) Warren, J. K. Evaporites through time: Tectonic, climatic and eustatic controls in marine and nonmarine deposits. *Earth-Sci. Rev.* **2010**, *98*, 217−268.
(49) Dela Pierre, F.; Natalicchio, M.; Ferrando, S.; Giustetto, R.; Birgel, D.; Carnevale, G.; Gier, S.; Lozar, F.; Marabello, D.; Peckmann, J. Are the large filamentous microfossils preserved in Messinian gypsum colorless sulfide-oxidizing bacteria? *Geology* **2015**, *43* (10), 855−858.
(50) Pellegrino, L.; Natalicchio, M.; Abe, K.; Jordan, R. W.; Longo, S. E. F.; Ferrando, S.; Carnevale, G.; Pierre, F. D. Tiny, glassy, and rapidly trapped: The nano-sized planktic diatoms in Messinian (late Miocene) gypsum. *Geology* **2021**, *49* (11), 1369−1374.
(51) Natalicchio, M.; Birgel, D.; Dela Pierre, F.; Ziegenbalg, S.; Hoffmann-Sell, L.; Gier, S.; Peckmann, J. Messinian bottom-grown selenitic gypsum: An archive of microbial life. *Geobiology* **2022**, *20* (1), 3−21.

https://doi.org/10.1021/acs.cgd.3c01124
Cryst. Growth Des. 2023, 23, 9094−9102